PERFORMANCE EVALUATION OF STANDING WAVE THERMOACOUSTIC ENGINES REGARDING HARMONIC SUPPRESSION

Caio Everton Carvalho Ribeiro Araujo[a*] and Flavio de Campos Bannwart[a]

[a]School of Mechanical Engineering - University of Campinas/UNICAMP
c216666@dac.unicamp.br, fcbannwart@fem.unicamp.br

ARTICLE INFO

***Keywords**: harmonics, resonance, standing wave thermoacoustic engine, thermoacoustics,*

Received: May 20, 2024
Reviewed: June 13, 2024
Accepted: June 28, 2024

ABSTRACT

This work consists of a comparative study between two standing wave thermoacoustic engines that differ in the geometry of their resonant chambers, but hold the same internal elements and operate at the same fundamental frequency and boundary conditions. One of the engines consists of a straight tube of circular cross-section as its main part that defines a resonant acoustic waveguide, while the other one consists of, in addition to a similar straight tube, also a conical bulb connected to one of its ends acting as a coupled Helmholtz resonator. According to the literature, the Helmholtz cavity causes a higher pitch quality in the first harmonic mode, which is of greatest interest from the energetic point of view. The main objective of this work is to verify and evaluate such an effect on the engine performance so that to explore its optimization by means of frequency and geometric. Both engines are simulated in the DeltaEC software. DeltaEC, however, does not include harmonics other than the fundamental one. Understanding of the influence of higher acoustic modes may lead to a better management of the thermoacoustic engine configuration towards higher thermal efficiencies.

1. INTRODUCTION

Thermoacoustics is a branch of acoustics that studies the thermoviscous interactions between gaseous resonant acoustic particle and solid substrate, so that the resulting heat transfer occurs in an orderly fashion. Depending on the heat transfers directions, the thermoacoustic cycle may perform as engine (prime-mover) or refrigerator. In the case of a thermoacoustic engine, acoustic oscillations are spontaneously generated within a porous material internal walls, called stack, as an irreversible process oriented to lower a previously imposed thermal potential along the stack.

Therefore, whenever a sufficiently high temperature gradient is established, thermal energy is converted into mechanical energy in the acoustic form as a consequence (Rott, 1980). Essentially, to ensure the onset temperature gradient, proper heat exchangers are to be installed at both stack ends (Swift, 1988).

Either standing or traveling waves may be generated within a thermoacoustic device, depending on its waveguide network configuration. For each case a suitable pore material can be chosen (Swift, 2002), and the corresponding thermoacoustic cycle can approach the Brayton or Stirling cycle regarding their respective efficiencies (Swift, 1988).

Among some important advantages of both types of thermoacoustic engines over the more traditional ones is the fact that they have no moving parts, nor do require mechanical sealing or lubrication; besides, despite of their lower thermal efficiency, thermoacoustic engines more are capable of regenerating energy from low-grade heat source, which is of sustainability value. Therefore, any progress towards this feature enhances a key potential for viable thermoacoustic engines; among them, mitigating harmful resonant modes standing wave engines employing Helmholtz resonators.

In this work, we investigate the relevance of harmonic modes higher than the fundamental one on the thermoacousticengine efficiency. Once the thermoacoustic effect is triggered, several harmonics are generated in addition to the first harmonic. These higher harmonics are integer

*Corresponding author: School of Mechanical Engineering - University of Campinas – UNICAMP
c216666@dac.unicamp.br

multiples of the fundamental frequency. *"One could imagine a deliberateuse of such harmonics to enhance some desired aspect of performance, but in our experience harmonics have only been harmful to system efficiency"* (Swift, 2017). According to the literature, such modes are harmful with respect to the engineefficiency, despite of its counter intuitiveness, as one would expect only contributive participation of each mode (Swift, 2017)

According to Yurii A. Ilinskii (1998), who studied standing wave thermoacoustic engines, conical and bulb-shaped resonators generate harmonics inefficiently because of dissonance, unlike cylindrical ones. This inefficiency in the generation of harmonics interests us enough to suppress them. Experiments have always supported this behavior, which have justified the use of harmonic suppressors so that to better tune the fundamental mode, of greater energetic interest; e.g. A. H. Ibrahim and Rahman (2013).

As an attempt to better investigate this harmful effect, we design and simulate two simple standing wave thermoacoustic engines in the software Design Environment for Low Amplitude ThermoAcoustic Energy Conversion (DeltaEC), from where the database used for analysis is extracted. One engine is essentially a straight waveguide and another one prevents the onset of the second harmonic by means the use of Helmholtz cavity.

This software numerically integrates Rott's acoustic wave propagation equation (Rott, 1980) in one dimension. The program allows manipulating thermophysical and geometrical in order to explore specific results. DeltaEC performs integrations using the shooting method along with guesses and targets. Guess and targets are resources that the program provides for handling unknown values based on known parameters established by the user. The convergence or divergence of simulations depend on the appropriate manipulation of guesses and targets, confronted with already defined boundary conditions.

Both thermoacoustic engines are designed based on the first-mode frequency of the porous material. We focus the investigation on the effects of the second harmonic. For that, the optimization of thermoacoustic engines through harmonic suppression is analysed. The thermoacoustic engines are compared for different geometries, kept the same boundary conditions. The difference in geometry is due to the presence of a Helmholtz resonator coupled to one of the engines. The Helmholtz resonator is a device that filters out unwanted harmonics in oscillations and favors the frequency range close to the first harmonic.

Ferro and Bannwart (2020) carried out tests with the DeltaEC software and verified the greater efficiency of thermoa-coustic engines operating at a single frequency, using the inverse matrix method. This work revealed parameters that were not obvious and allowed an investigation and exploration of other variables based on them, as well as an improvement in the efficiency of the thermoacoustic engine.

The objectives of this work are to verify and evaluate the benefit of harmonic suppression by means of simulations and experiment, confronted with analytical modeling. A test rig is being designed and built aiming to provide unequivocal evidence of the effect.

2. DEVELOPMENT

2.1 Harmonic Generation

The Navier-Stokes equation from fluid mechanics, represented here by Eq. (1), contains terms that can generate harmonics and contribute to non-linear effects.

$$\rho\left(\frac{\partial V}{\partial t} + V\cdot\nabla V\right) = -\nabla P + \nabla\cdot\vec{\vec{\sigma}} \qquad (1)$$

Where the term $\frac{\partial V}{\partial t}$ is the change in velocity with time, $V\cdot\nabla V$ is the convective term, and ∇P is the pressure gradient.

In Eq.1, the term $\vec{\vec{\sigma}}$ is the stress tensor composed of nine shear stress components. Generally, gradients caused by viscosity can be negligible, and fluid motion can be treated as incompressible when we consider the effects of momentum.

With these approximations, Eq.(1) can be simplified to:

$$\rho\left(\frac{\partial V}{\partial t} + V\cdot\nabla V\right) = -\nabla P + \mu\nabla^2 V \qquad (2)$$

or

$$\rho\left(\frac{\partial u}{\partial t} + u\frac{\partial u}{\partial x} + v\frac{\partial u}{\partial y} + w\frac{\partial u}{\partial z}\right) = -\frac{\partial P}{\partial x} + \\ + \mu\left(\frac{\partial^2 u}{\partial x^2} + v\frac{\partial^2 u}{\partial y^2} + w\frac{\partial^2 u}{\partial z^2}\right) \qquad (3)$$

In the x direction:

$$\rho\left(\frac{\partial u}{\partial t} + u\frac{\partial u}{\partial x}\right) = -\frac{\partial P}{\partial x} + \frac{\partial^2 u}{\partial x^2} \qquad (4)$$

This approximation is more than sufficient to deal with thermoacoustic problems (Swift, 2017).

The term responsible for the generation of harmonics is contained in $\frac{\rho\,\partial V}{\partial t}$, or $\frac{\rho\,\partial u}{\partial t}$, in the x direction only. To obtain this term, consider Rott's

acoustic approximations, in which the wave propagates only in the x direction and therefore the velocity is: $V = u \cdot i$, because v and w are zero. Writing ρ and u in complex notation, we have:

$$\rho = \rho_m + \rho_1,$$
$$u = u_1$$

Where the subscript 1 means complex variable and correspond to the acoustic fluctuation.

Considering only the real parts of ρ and u, we can write:

$$\rho = \rho_m + \rho_1 \cos(\omega t),$$
$$u = -\omega \xi_1 \sin(\omega t).$$

Where u_1 and ξ_1 are the complex amplitudes of velocity and displacement, respectively.

Developing the term $\frac{\rho \partial V}{\partial t}$ we get the following expression:

$$[\rho_m + \rho_1 \cos(\omega t)] \times [-\omega^2 \xi_1 \cos(\omega t)],$$
$$-\rho_m \omega^2 \xi_1 \cos(\omega t) - \rho_1 \omega^2 \xi_1 \cos(\omega t) \cos(\omega t)$$

$$[\rho_m + \rho_1 \cos(\omega t)] \times \frac{\partial}{\partial t} [-\omega \xi_1 \sin(\omega t)],$$

From trigonometric identity:

$$\cos(\omega t) \cos(\omega t) = \frac{1}{2} [1 + \cos(2\omega t)]$$

According to Swift (2017), once a frequency 2ω is present, its interaction with the fundamental oscillations ω occurs via nonlinear terms, and consequently these terms leads to waves with oscillations at 3ω because $\cos(\omega t) \times \cos(2\omega t) = \frac{1}{2} [\cos(2\omega t)] \times \cos(2\omega t)]$. Therefore, in accordance with experimental observation, Swift (2017) concluded that higher har monic modes impair the efficiency of thermoacoustic engines.

2.2 The Helmholtz Resonator

The Helmholtz resonator is a volume V with rigid walls and a neck of area A and length L that can be modeled as lamped-parameter. In this work, the Helmholtz resonator is used to filter frequencies close to the first harmonic and eliminate unwanted harmonics. The following formula determines your resonant frequency:

$$f = \frac{c}{2\pi} \sqrt{\frac{A}{L'V'}} \quad (5)$$

Where c is the speed of sound, A is the neck area and V is the volume of the bulb.

Equation 5 is not suitable for calculating the resonator parameters in thermoacoustic engines, as it was obtained for empty tubes under different conditions.

In the development of Eq. 5 the waveguide provides an inertance and the bulb volume provides a compliance. Reactance is the imaginary part of impedance, and here in the tube-sphere system, it depends on the combination of inertance and compliance. The resonance condition occurs when the reactance goes to zero, resulting in Eq. 5.

However, in thermoacoustic engines, the waveguide contains heat exchangers and a porous material, which provide some kind of resistance that was not considered in the development of this equation. The results obtained by the simulations in DeltaEC do not correspond with the results obtained analytically by Eq. 5.

2.3 Stack

The component that maintains the temperature gradient in the oscillating fluid is the porous material, the heart of the thermoacoustic engine. This component has some essential characteristic lengths. One of them is the thermal penetration depth, which was used to dimension the thermoacoustic engine.

The thermal penetration depth is a characteristic length that is perpendicular to the direction of fluid motion. This length measures how far heat can diffuse sideways during a time interval of the order of the oscillation period divided by π. Its expression is given by Eq. 6.

$$\delta_\kappa = \sqrt{\frac{2K}{\omega \rho c_p}} \quad (6)$$

Where δ_κ is the thermal penetration depth, K is the thermal conductivity, c_p is the specific heat at constant pressure and ρ is the specific mass.

According to Russell and Weibull (2002), the idea is that the walls of the porous material have a layer separation of approximately four times δ_κ. Using this approximation together with the dimensions of the porous material, obtained experimentally, we determined δ_κ= 0.25mm.

The porous material used in this work has a pore density of 400 CPSI and, through experimental measurements, the internal dimension of the pore is a square with side equal to 1mm and porosity equal to 0.62.

One of our goals is to build these engines in the university laboratory, for that we use the properties of air in the standard state of 25ºC and 1 atmosphere of pressure to make the project viable. The frequency obtained from these data for the porous material is f = 110Hz.

3. DELTAEC MODELING

Nikolaus Rott was the first to derive correct expressions for motion, pressure, and energy transport in a channel with small sinusoidal oscillations and a temperature gradient. He proposed (Rott, 1969) the model described by Eq.(7):

$$\left(1+\frac{(\gamma-1)f_\kappa}{1+\epsilon_S}\right)p_1+\frac{p_m a^2}{\omega^2}\frac{d}{dx}\left(\frac{1-f_v}{p_m}\frac{dp_1}{dx}\right)-$$

$$+\beta\frac{a^2}{\omega^2}\frac{f_\kappa-f_v}{(1-\sigma)(1+\epsilon_S)}\frac{dT_m}{dx}\frac{dp_1}{dx}=0 \qquad (7)$$

which can be rewritten as two first-order coupled equations

$$\frac{dp_1}{dx}=-\frac{i\omega\rho_m}{A(1-f_v)}U_1 \qquad (8)$$

$$\frac{dU_1}{dx}=-\frac{i\omega A}{\rho_m a^2}+\left(1+\left(\frac{(\gamma-1)f_\kappa}{1+\epsilon_S}\right)p_1+\right.$$

$$+\frac{(f_\kappa-f_v)}{(1-\sigma)(1+\epsilon_S)}\beta\frac{dT_m}{dx}U_1 \qquad (9)$$

where f_v and f_x are complex variables that depend on the properties of the gas and the size and shape of the pores, ϵ_s is the correction factor for finite solid heat capacity, τ is the Prandtl number, β is the thermal expansion coefficient, ω is the angular frequency, ρ_m is the average density, γ is the ratio of specific heats, A is the cross-sectional area, U_1 is the volume flow rate, α is the sound speed, T_m is the average temperature and p_1 is the complex pressure.

From fluid mechanics, the momentum equation gives rise to Eq. (8), and the continuity equation gives rise to Eq. (9).

DeltaEC uses Eqs. (8) and (9) to perform numerical integrations across the segments that make up the system.

The capabilities and restrictions of this software that were used in this work is discussed below.

In this session the main characteristics of the computational system that will be used to observe the behavior of thermoacoustic engines for different geometries are presented. For comparison purposes, both engines operate under the same working conditions and have the same thermoacoustic core, which consists of a hot heat exchanger (HHX), porous material (STACK), and ambient heat exchanger (AHX). The working fluid is air operating at a pressure of 1 atmosphere and a temperature of 630K.

For the thermoacoustic engines to be in harmony with the speed of sound, the frequency, and the wavelength of the porous material, they were designed with a wavelength compatible with the frequency of the stack. To design the thermoacoustic engines, the porous material thermal penetration depth equation was used as a database. With the pressure and temperature conditions of the laboratory, it was determined that the optimal frequency for the stack was 110Hz. Thus, to be in tune with the porous material, the two engines must operate at the same working frequency.

In this work, experimental computational models were developed for two thermoacoustic engines: one with a constant cross-sectional area along the entire length of the waveguide, here called Straight Engine (Figs. 1 and 2), and an engine with a cone and a spherical bulb at one end, called a bulb engine (Figs. 5 and 6). The models and methods used in this work are detailed below.

3.1. STRAIGHT ENGINE AND BULB ENGINE

We will now deal with the main models of thermoacoustic engines studied in this work. These models were developed with a view to their construction for future experiments.

The first step adopted to model thermoacoustic engines was to obtain the optimal frequency for the porous material that will be used in future experiments. Once we know the ideal working frequency, we define it as a guess so that we can dimension the lengths in order to obtain a frequency close to the stack frequency. In the case of the bulb engine, the dimensions of the Helmholtz resonator must be considered in the sizing, as they directly influence the system frequency.

The hot and cold heat exchangers are maintained at 600K and 298K, respectively, and their temperatures are defined as targets. In the software, the number of guesses needs to be equal to the number of targets; therefore, to correspond to these last two mentioned targets, we define the heat fluxes that enter and leave the system as guesses. Finally, at the end of the models, there is no air leakage; that is, the models are sealed, and there is no mass flow crossing the system boundary. In DeltaEC, this condition can be established by inserting a segment called HARDEND together with two targets.

To match these last-mentioned targets, we define the volume velocity modulus and the frequency as guesses in the initial BEGIN segment. Next, we will show the configurations obtained for thermoacoustic engines based on the criteria mentioned above.

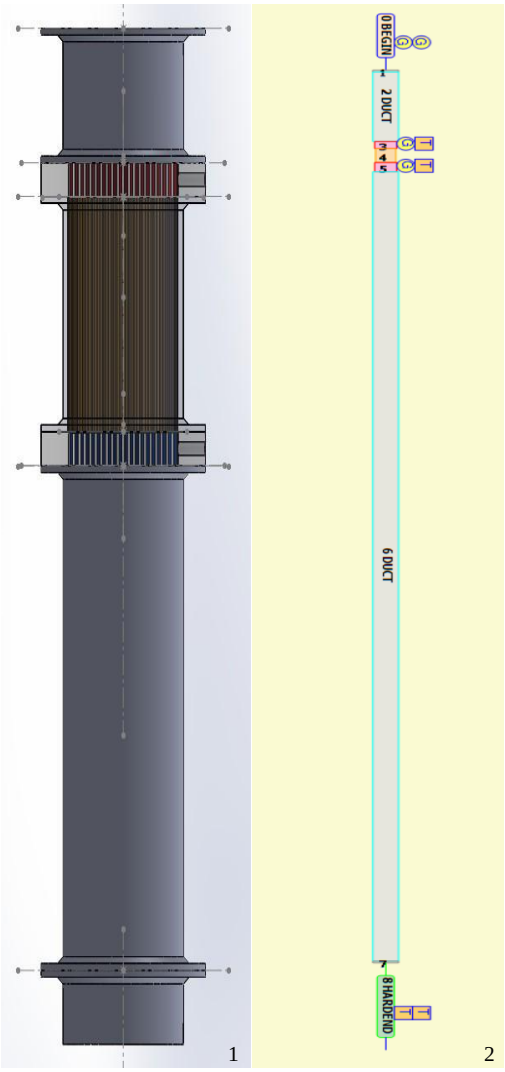

Figure 1. Straight Engine (SolidsWorks);
Figure 2. Scheme of the Straigth Engine (DeltaEC)

3.1.1. STRAIGHT ENGINE

The main feature of the straight engine is a constant cross-sectional area throughout its longitudinal length and is com- posed of the following elements: BEGIN, SURFACE, DUCT1, HHX, STACK, AHX, ANCHOR, DUCT2, SURFACE, and HARDEND as shown in Fig. 2. The global variables are defined in the BEGIN segment with the following values: 1atm, 450K, 0º of phase between p_1 and u_1, and |U| as a being guess. The hot and cold heat exchanger temperatures are defined as targets, and their values are 600K and 298K, respectively; its porosity was defined as 0.75; and their lengths are 0.015m and 0.02m. The lengths of the waveguides are 2DUCT = 0.15m and 6DUCT = 1.7m , and their diameter was defined as 40mm. The materials chosen to compose the heat exchangers and the STACK are copper and ceramic, respectively; the other segments are made of ideal materials.

In Fig. 3 we can see the temperature profiles of the gas and the solid parts of the heat exchangers. The temperature gradient in the gas occurs in element 4, which is the stack, located between elements 3 and 5, which are the hot and cold heat exchangers, respectively (Fig. 2). This gradient is represented in Fig. 3 by a slight slope in the green line, and it is caused by the extreme temperatures of the hot and cold heat exchangers, represented by the black dotted line. The heat fluxes entering and leaving the system through HHX and AHX are defined as guesses.

The ANCHOR segment replaces the standard thermal insulation of the segments with a system that treats them as if they were immersed in a thermal bath at the same temperature as the local gas, and this affects the dissipation of Htot, as can be seen in Fig. 3, where the Htot curve tends to zero in the regions after the thermoacoustic core.

At the end of the model, to establish a sealing condition, we define the real and imaginary parts of the normalized impedance as targets in the HARDEND segment. It can be seen in Fig.3 that the acoustic power (E_{dot}) is zero at the end of the model and in Fig. 4 where the |U| is zero at the end of the model. To match these last two targets, we define the volume velocity modulus and frequency in the BEGIN segment as guesses.

The production of acoustic power occurs due to the fact that the |U| and the |p| are different from zero in the initial segment of the model and their phases are not orthogonal, as can be seen in Fig. 4. This can also be seen in Fig. 3, where the acoustic power is at its maximum at the beginning of the model.

3.1.2. BULB ENGINE

Unlike the Straight Engine, the Bulb Engine does not possess a constant cross-sectional area along its length; it has at one of its ends a cone and a spherical bulb coupled to the waveguide. These last elements constitute the Helmholtz resonator. This engine consists of the following elements: BEGIN, SURFACE, DUCT, HHX, STACK, AHX, ANCHOR, DUCT, CONE, COMPLIANCE, and HARDEND as shown in Fig. 6.

The global parameters are defined in BEGIN, and their values are 1atm, 450K, 0º of phase for p_1 and u_1, and |U| as a guess. The hot and cold heat exchanger temperatures are defined as targets, and their values are 600K and 298K, respectively; its porosity was defined as 0.75; and their lengths are 0.015m and 0.02m. The geometric parameters of the elements are: 2DUC = 0.15m, 6DUCT = 1.22m (with diameter defined as 40mm), CONE = 0.005m (input area 1.2566 x $10^{-3}m^2$; output area 4, 035 x $10^{-3}m^2$), and COMPLIANCE= 5.5 x $10^{-4}m^3$. The materials chosen to compose the heat exchangers and the STACK are copper and ceramic, respectively; the other segments are made of ideal materials.

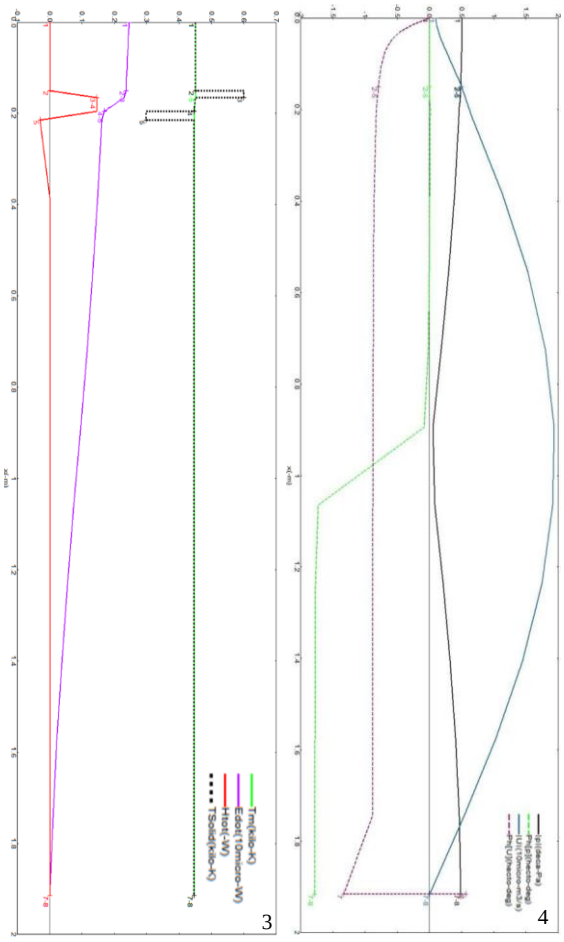

Figure 3. Temperature of the gas (green) an solid parts (dotted black), acoustic power (purple) and total power (red) profiles of the Straight Engine;
Figure 4. Acoustic pressure amplitude (black) and phase (green), and acoustic volume velocity amplitude (gray) and phase (dashed lilac) profiles of the Straight Engine

In Fig.7 we can see the temperature profiles of the gas and the solid parts of the heat exchangers. The temperature gradient in the gas occurs in element 4, which is the stack, located between elements 3 and 5, which are the hot and cold heat exchangers, respectively (Fig. 6). This gradient is represented in Fig. 7 by a slight slope in the green line, and it is caused by the extreme temperatures of the hot and cold heat exchangers, represented by the black dotted line. The heat fluxes entering and leaving the system through HHX and AHX are defined as guesses.

The effect of the Helmholtz resonator can be seen in Fig. 8, where the curve that expresses the |U| undergoes an instantaneous reduction exactly at the point where the resonator is positioned.

The ANCHOR segment replaces the standard thermal insulation of the segments with a system that treats them as if they were immersed in a thermal bath at the same temperature as the local gas, and this affects the dissipation of Htot, as can be seen in Fig. 7, where the Htot curve tends to zero in the regions after the thermoacoustic core.

At the end of the model, to establish a sealing condition, we define the real and imaginary parts of the normalized impedance as targets in the HARDEND segment. And this can be seen in Fig.7 where the acoustic power (E_{dot}) is zero at the end of the model and in Fig.8 where the |U| is zero at the end of the model. To match these last two targets, we define the volume velocity modulus and frequency in the BEGIN segment as guesses.

The production of acoustic power occurs due to the fact that the |U| and the |p| are different from zero in the initial segment of the model and their phases are not orthogonal, as can be seen in Fig. 8. This can also be seen in Fig. 7, where the acoustic power is at its maximum at the beginning of the model.

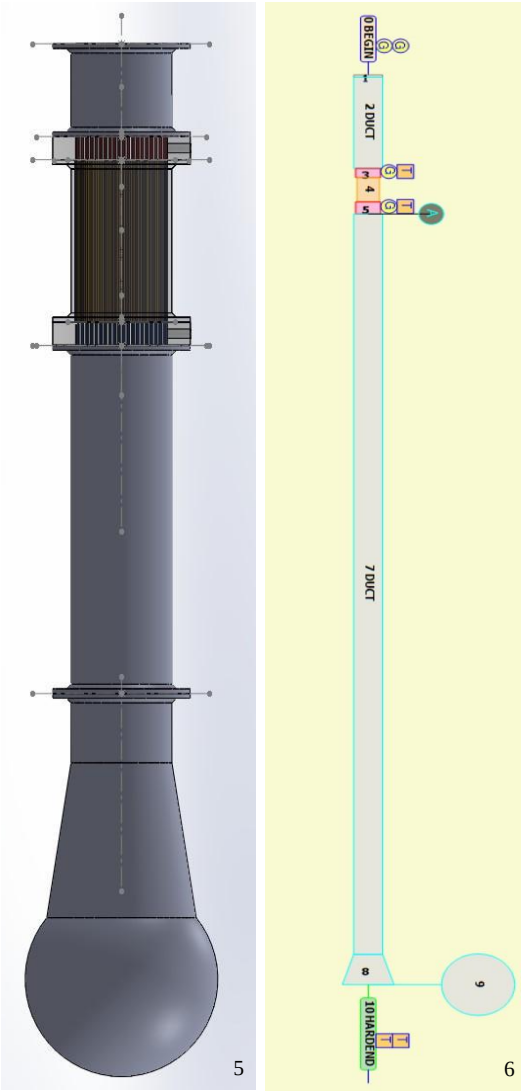

Figure 5. Bulb Engine (SolidWorks);
Figure 6. Bulb Engine (DeltaEC).

3.2. RESTRICTION TO THE FIRST HARMONIC

An important restriction of the DeltaEC, which has been on focus of this work, is the fact that it only works with the first harmonic. This makes the software unfeasible for checking the effects of higher harmonics or their suppression (filtering), which can done in a test rig by means of a Helmholtz resonator. Therefore, we make a strategic use of the DeltaEC so that to aid in revealing such effects.

3.3. SIMULATION RESULTS

3.3.1. THERMOVISCOUS EFFECTS

For the engines to operate at the ideal frequency of the porous material, their longitudinal lengths were set arbitrarily. The results obtained for the engines operating under the same working conditions and at the ideal frequency of the porous material reveal that the Bulb Engine reaches such a frequency decreasing its length.

Along the development of thermoacoustic engines, some models were made with different configurations of guesses and targets. These models had their length defined as guess and their frequency defined as target, equal to 110Hz. The results of these settings also show a decrease in the linear length of the Bulb Engine.

3.3.2. HELMHOLTZ RESONATOR

In addition to the Helmholtz resonator interfering with the waveguide length to keep the system at a proper frequency, it also interferes with the|U|. Through the simulations, it can be seen that the volume of the bulb is inversely proportional to |U|, which was defined as a guess in the initial BEGIN segment. The acoustic power produced by a thermoacoustic engine is given by the following equation:

$$E_{dot} = \frac{1}{2}|p_1||U_1|\cos(\phi_p U)$$

Where $\cos(\phi_p U)$ is the cosine of the phase difference between p and U. Through this expression, we can see that the acoustic power can be changed according to the volume of the bulb.

3.3.3. FORCED SECOND HARMONIC

In an attempt to simulate the effects of the second harmonic, some analyses were conducted with a frequency of 220Hz, which is an integer multiple of the first harmonic. Within this frequency change, we obtain a reduction in the acoustic power produced by the system.

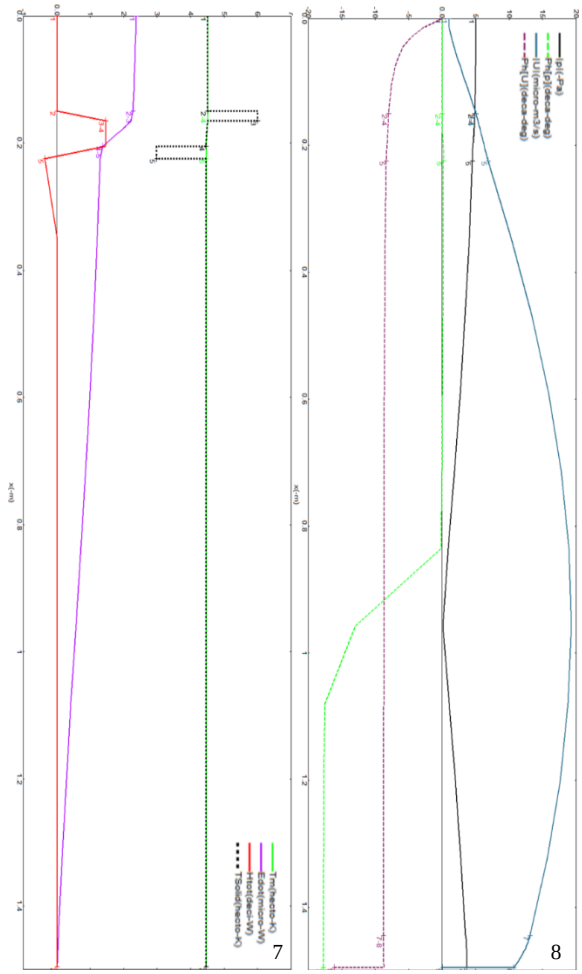

Figure 7. Temperature of the gas (green) an solid parts (dotted black), acoustic power (purple) and total power (red) profiles of the Bulb Engine;
Figure 8. Acoustic pressure amplitude (black) and phase (green), and acoustic volume velocity amplitude (gray) and phase (dashed lilac) profiles of the Bulb Engine

4. FUTURE ANALYSIS

The methodology that will be addressed in the future in this work aims, through a practical experiment, to investigate the suppression of harmonics performed by the Helmholtz resonator. As the DeltaEC has the aforementioned restrictions, the suppression of harmonics cannot be verified by it, so we will do experiments to study these effects.

This document shows the dimensions of the thermoacoustic engines that will be built. The waveguides will be made of PVC tube with an internal diameter of 40mm. In the region of the hot heat exchanger, the tube must be metallic to withstand high temperatures. The porous material is a ceramic car catalyst, which must be tailored to fill the inner cylindrical region of the tube and has a pore density of 400 CPSI. The cold heat exchanger will be made of

copper tubes in a transverse position to the waveguide. The Helmholtz resonator will have its dimensions estimated by the SolidWorks software, and its assembly will be made with PVC sheets. Part seals are under discussion.

Heat will be added to the system by a nickel-chromium electrical resistance, which will have a potentiometer to regulate the heat flows and adapt them to the problem. To remove heat from the system, a fluid will be pumped through the copper tubes in the cold heat exchanger.

The fluids that will remove heat from the system will initially be water and later iron fluid. The behavior of fluid iron will be analyzed in a work that is being developed in parallel, referring to thermomagnetism.

Both thermoacoustic engines will be receiving the same input power. Thus, they will have identical working condi- tions, as they will be in the same pressure and temperature environment.

The signals will be read at the left end of the engines, which corresponds to segment 1 (SURFACE) in Figs. 2 and 6. We intend to collect the data with some kind of microphone and process it with Matlab software.

Together with the experiments, the analytical development of the thermoacoustic equations will also be carried out, so that we can validate, through simulation software (Matlab or Comsol), the correspondence between the results of the practical experiments and the analytical development and, thus, obtain more accurate results on harmonic suppression.

5. CONCLUSION

This work aims to analyze the effects of harmonic suppression in standing-wave thermoacoustic engines. For this, two thermoacoustic engines with different geometries were developed: one with a Helmholtz resonator coupled to the waveguide and another without this resonator. The simulations were done in the DeltaEC software, which is limited to the first harmonic, and this makes the program unsuitable for verifying these effects.

Due to the DeltaEC restrictions, some hypotheses were raised to explain the detrimental behavior of higher harmonic harmonics: (1) The second harmonic has less energy because it divides the generated acoustic power with the first har- monic and is less efficient because it is at a higher frequency, making it less suitable for porous material. (2) Nonlinearities in dynamic systems in general, present at higher harmonics, are usually associated with energy dissipation in the form of heat, which impairs efficiency in the second mode. (3) Higher harmonics impair the thermal efficiency of the cyclic mo- tion of the acoustic particle at the fundamental frequency, reducing the contrast in velocity and pressure when comparing extreme and central positions.

Some results were obtained through simulations carried out for the second harmonic harmonic; such results are associated with hypothesis (1). Even if DeltaEC assumes that the second harmonic is the only existing frequency in the system, as it only works with one frequency, it reveals a worsening in the production of acoustic power, and this is in agreement with hypothesis (1).

Other results showed that the engine with the Helmholtz resonator becomes more efficient because the resonator directly affects the system frequency, which causes a reduction in the waveguide length. This reduction, consequently, reduces the thermoviscous effect, minimizing the losses due to the direct contact of the gas with the solid walls inside the waveguide.

A test rig is under development aiming to better understand the harmonic suppression and to evaluate our hypotheses that have been made so far. This work will also serve as parameter for future works that will involve a thermomagnetism context in the cold heat exchanger.

6. REFERENCES

A. H. Ibrahim, M. Shaaban, H.O. and Rahman, E.A., 2013. “Suppressing harmonics in standing-wave thermoacoustic engines”.

Ferro, B. and Bannwart, F.C., 2020. “Modeling a thermoacoustic engine under rott’s approach from experimental transfer matrices of a thermoacoustic core”. *Brazilian Congress of Thermal Sciences and Engineering*.

Rott, N., 1980. “Thermoacoustics”. *Advances in Applied Mechanics*, Vol. 20, pp. 135–175.

Rott, N., 1969. “Damped and thermally driven acoustic oscillations in wide and narrow tubes”. *Journal of Applied Mathematics and Physics (ZAMP)*, Vol. 20, p. 230–243.

Russell, D.A. and Weibull, P., 2002. “Tabletop thermoacoustic refrigerator for demonstrations”. *Am. J. of Physics*, Vol. 70, pp. 1231–1233.

Swift, G.W., 1988. “Thermoacoustic engines”. *Acoustical Society of America*, Vol. 84, pp. 1145–1180.

Swift, G.W., 2002. *Thermoacoustics: A unifying perspective for some engines and refrigerators*. Acoustical Society of America, Melville, NY.

Swift, G.W., 2017. *Thermouacoustic*. Los Alamos, New Mexico, USA.

Yurii A. Ilinskii, Bart Lipkens, T.S.L., 1998. “Nonlinear standing waves in an acoustical resonator”. *Acoustical Society of America*, Vol. 104, p. 2664.

7. RESPONSIBILITY NOTICE

The authors are solely responsible for the printed material included in this paper.